Application of lateral shearing interferometry to stochastic inputs*

Ronald R. Gruenzel
Air Force Avionics Laboratory, Wright-Patterson Air Force Base, Ohio 45433
(Received 10 June 1976)

Lateral shearing interferometry is a simple and accurate method of measuring the shape of an optical wave front. However, the complex mathematics required in reduction of the interferograms has limited the adoption of this interferometric technique. A data reduction technique using Fourier analysis methods has been developed which makes lateral shearing interferogram reduction more flexible. This technique is hypothetically applied to the measurement of wave fronts propagating through a turbulent medium, and demonstrates the simplicity and accuracy of this data reduction method.

INTRODUCTION

Wave-front shearing interferometry[1] provides a simple and accurate means for testing the shape of wave fronts. However, the complex mathematics required for data reduction[2–5] has limited the adoption of the technique. One simple but accurate technique[6] has been devised, but it is dependent on evaluation at shear distances.

A data reduction technique using Fourier analysis methods has been developed which makes lateral shearing interferometric data reduction more flexible. Results can now be obtained by performing a Fourier transformation of the sheared wave-front data, a proper filtration in the frequency domain, and an inverse transformation to obtain the shape of the wave front. The result is an accurate determination of the wave-front deviations from a best fitting reference sphere. The restriction of evaluation at only shear distances is not required by this data reduction technique. However, evaluation must be performed at equally spaced points in the interferogram.

This technique is especially well suited for lateral shearing interferometric measurements of stochastic processes, such as wave-front deformations introduced by random polishing errors of optical surfaces and/or propagation through a turbulent atmosphere. The Fourier analysis approach easily permits calculation of the power spectrum or autocorrelation function of the stochastic process as part of the data reduction technique and therefore can determine an important statistical parameter of the process. Since the wave-front shape is also reconstructed by this data reduction technique, the probability density function is also derivable from the data.

BACKGROUND

The lateral shearing interferometer gives the difference in aberration at pairs of points separated by the shear. When the shear is small, the resulting interferogram is approximately the directional derivative of the aberration. It has proven to be a most useful instrument, but for some users it is unpopular, as it does not give the wave aberration directly but only differences.

The main disadvantages of this type of interferometer are the following: no sensitivity to wave-front shapes perpendicular to the shear direction; the interferogram covers only part of the aperture; no sensitivity to periodic errors having a period equal to the shear in a direction parallel to it. However, if the shear is small, periodic errors equal to the shear are unlikely to be present, and interferograms can be recorded in which the shear is at right angles to its direction in the first case.

The sheared interferograms are usually interpreted by integration of the wave-front slope. If the shear is in the x direction and the shear is Δx, the aberration at x for one component meets the aberration at $x+\Delta x$ for the other. Hence, since the aberration of a wave front is expressible as a function of x and y, $W(x, y)$, then by Taylor's theorem,

$$W(x+\Delta x,\ y) = W(x,\ y) + \Delta x\ \frac{\partial W}{\partial x} + \frac{(\Delta x)^2}{2!}\ \frac{\partial^2 W}{\partial x^2} + \cdots . \tag{1}$$

If the shear is small and the rate of change of $\partial W/\partial x$ is not large, the $(\Delta x)^2$ term in Eq. (1) is negligible in comparison to Δx, and

$$W(x+\Delta x) - W(x,\ y) = \Delta x \frac{\partial W}{\partial x} \quad . \tag{2}$$

As the aberration difference grows, the vertical displacement of the fringe tells us the retardation difference in so many wavelengths, x_λ, on the scale of the interferogram. Hence the slope of the wave front is given by

$$\frac{\partial W}{\partial x} = \frac{W(x+\Delta x,\ y) - W(x,\ y)}{\Delta x} = \frac{x_\lambda}{\text{shear}} \quad , \tag{3}$$

and

$$W(x,\ y) - W(x_0,\ y) = \int_{x_0}^{x} \frac{x_\lambda}{\Delta x}\, dx \ , \tag{4}$$

where $W(x_0, y)$ is the aberration at the reference point (x_0, y) selected for the interferogram.

The aberration of the wave front is therefore obtained by an integration of the area under a curve showing the number of fringes per unit distance in the direction of shear, and this simplification is only possible when the shear is small and the rate of change of $\partial W/\partial x$ is not large. More complex data reduction techniques are required when these conditions are not satisfied.

MEASUREMENT OF STOCHASTIC INPUTS

The effects of atmospheric turbulence on the propagation of optical wave fronts have been interferometrically investigated by many authors. Specifically, Michel-

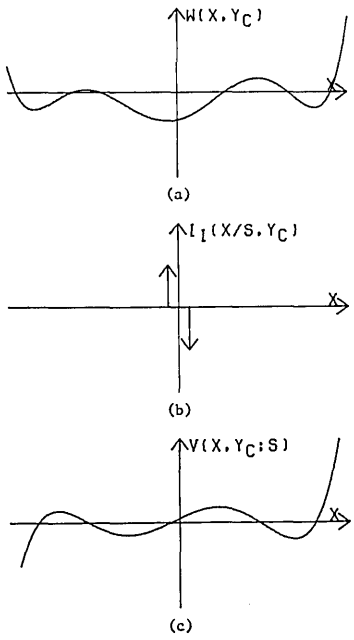

FIG. 1. Wave-front shape, odd-impulse pair function, and resultant lateral shearing aberraltion differences.

son,[7,8] Mach-Zender,[9,10] reversing front,[11,12] grating,[13] differential,[14] channel spectrum,[15] correlation,[16,17] and phase difference interferometers,[18,19] have been used to measure the phase fluctuations of the stochastic process.

Since the nature of the problem precludes the use of a plane reference wave front, a lateral shearing interferometer is ideally suited for measurements of the effects of atmospheric turbulence on optical wave-front propagation. Using this interferometric approach a reference beam is provided by the propagating wave front. The wave-front shape can be reconstructed from the interferogram using the Fourier data reduction technique, and a complete statistical analysis, including determination of the probability distribution of the random process, is experimentally obtainable.

THEORETICAL CONSIDERATIONS OF FOURIER DATA REDUCTION TECHNIQUE

A lateral shearing interferogram of a wave front of infinite extent propagating through a turbulent medium can be written as

$$V(x,\ y;\ s) = W\left(x+\frac{s}{2},\ y\right) - W\left(x-\frac{s}{2},\ y\right) \tag{5}$$
$$= W(x,\ y) * \frac{2}{s} I_I\left(\frac{x}{s}\right),$$

when the shear, s, is in the x direction. The "$*$" represents a convolution operation, and $I_I(x/s) = \frac{1}{2}\delta[(x/s)+\frac{1}{2}] - \frac{1}{2}\delta[(x/s)-\frac{1}{2}]$ is an odd-impulse pair function.[20]

Equation (5) is a convolution integral of the x component of the wave-front shape, $W(x, y)$, shown in Fig. 1(a) for a section, $y = y_c = a$ constant in the interferogram, with an odd-impulse pair function, shown in Fig. 1(b). This integral represents the difference in phase at pairs of points separated by the shear for an infinite continuous record and is shown in Fig. 1(c) for the wave front of Fig. 1(a). For small shears, this integral is approximately the directional derivative of $W(x, y_c)$. Since this integral is a convolution integral, its Fourier transform is, by the convolution theorem,[20]

$$\tilde{V}(\xi,\ \eta;\ s) = \tilde{W}(\xi,\ \eta)\, 2i \sin(\pi s \xi)\ , \tag{6}$$

where ξ and η are the x and y spatial frequencies, respectively, the "~" denotes a functions Fourier transform representation, and $2i\sin(\pi s\xi)$ is the Fourier transform of $(2/s)I_I(x/s)$.

Solving Eq. (6) for $\tilde{W}(\xi, \eta)$ we obtain

$$\tilde{W}(\xi,\ \eta) = \tilde{V}(\xi,\ \eta;\ s)/2i\sin(\pi s\xi)\ . \tag{7}$$

Since

$$W(x,\ y) = \mathfrak{F}^{-1}[\tilde{W}(\xi,\ \eta)]\ , \tag{8}$$

where $\mathfrak{F}^{-1}$ is the inverse Fourier transform operation,

$$W(x,\ 0) = \mathfrak{F}_x^{-1}\left[\int_{-\infty}^{+\infty} \tilde{W}(\xi,\ \eta)\, d\eta\right]\ , \tag{9}$$

where $\mathfrak{F}_x^{-1}$ is the x inverse Fourier transform operation.

Substituting Eq. (7) into Eq. (9),

$$W(x,\ 0) = \mathfrak{F}_x^{-1}\left\{\frac{\int_{-\infty}^{+\infty} \tilde{V}(\xi,\ \eta;\ s)\, d\eta}{2i\sin(\pi s\xi)}\right\} \tag{10}$$
$$= \mathfrak{F}_x^{-1}\left\{\frac{\mathfrak{F}[V(x,\ 0;\ s)]}{2i\sin(\pi s\xi)}\right\}\ ,$$

and we recover the wave-front shape, $W(x, 0)$.

Although the above derivation was performed for the section $y = 0$ in the interferogram, it can be seen that the same arguments hold for any section $y = y_c$ in the interferogram.

For a lateral shearing interferogram of finite extent measured at intervals Δx along a section $y = y_c$ in the record, Eq. (5) is equivalent to a lattice of samples of the function, $W(x + s/2,\ y_c) - W(x - s/2,\ y_c)$. Omitting in the notation the functional dependence on y,

$$V_s(x;\ s) = \left\{\left[\mathrm{rect}\left(\frac{x}{X}\right) V(x;\ s)\right] \frac{1}{\Delta x}\ III\left(\frac{x}{\Delta x}\right)\right\} * \frac{1}{X}\ III\left(\frac{x}{X}\right), \tag{11}$$

where $X = N\Delta x$ is the maximum length of the interferometric data record, $\mathrm{rect}(x)$ is the rectangle function,[20] and $III(x) = \sum_{-\infty}^{+\infty} \delta(x-n)$ is the sampling or replicating function.[20] The function $(1/\Delta x)III(x/\Delta x)$ samples, and the rectangle function truncates the infinite continuous record, $V(x;\ s)$. The function $(1/X)III(x/X)$ produces periodic replicas of the truncated, sampled interferogram, which is necessary for application of the fast Fourier transform algorithm.[21]

Substituting Eq. (5) into Eq. (11),

$$V_s(x;\ s) = \left(\left\{\mathrm{rect}\left(\frac{x}{X}\right)\left[W(x) * \frac{2}{s} I_I\left(\frac{x}{s}\right)\right]\right\} \frac{1}{\Delta x}\ III\left(\frac{x}{\Delta x}\right)\right)$$
$$* \frac{1}{X}\ III\left(\frac{x}{X}\right)\ . \tag{12}$$

Fourier transforming Eq. (12) we obtain

$$\tilde{V}_s(\xi;\ s) = X[(\{\mathrm{sinc}(X\xi) * [\tilde{W}(\xi)\, 2i \sin(\pi s \xi)]\} * III(\Delta x \xi))\, III(X\xi)] , \tag{13}$$

where $\mathrm{sinc}(x) = \sin(\pi x)/\pi x$, and a smoothed sampled spectrum of $W(x) * (2/s) I_I(x/s)$ is erected about each point $n/\Delta x$ on the ξ axis.

Now, from the sampling theorem,[22–24] if this spectrum is "band limited," we can multiply Eq. (13) by an appropriate rectangle function, specifically, $\mathrm{rect}(\Delta x \xi)$, and if Δx has been chosen sufficiently small to prevent aliasing in the frequency domain, the zero order of this spectrum can be filtered out to obtain

$$\tilde{V}_s(\xi;\ s) = \mathrm{rect}(\Delta x \xi)[(\{X \,\mathrm{sinc}(X\xi) * [\tilde{W}(\xi) 2i \sin(\pi s \xi)]\} * III(\Delta x \xi))\, III(X\xi)] . \tag{14}$$

Equation (14) can be compared with the Fourier transform of the sampled, replicated, and filtered infinite continuous wave-front function forming the lateral shearing interferogram,

$$\tilde{W}_s(\xi) = \mathrm{rect}(\Delta x \xi)[\tilde{W}(\xi) * III(\Delta x \xi)]\, III(X\xi) . \tag{15}$$

If the sinc function of Eq. (14) is sufficiently narrow so that appreciable smoothing does not occur when the convolution is performed, $\tilde{W}_s(\xi)$ can be obtained from $\tilde{V}_s(\xi;\ s)$ by dividing the zero order of each sampled value of $\tilde{V}(\xi;\ s)$ at spatial frequency ξ by the appropriate value of $2i \sin(\pi s \xi)$. This restriction requires a long enough record length, represented by the rectangle function of Eq. (12), so that the sinc function is narrow in its spatial frequency width compared to the fine detail of the wave front's Fourier transform. Therefore, with this approximation,

$$\tilde{W}_s(\xi) = \tilde{V}_s(\xi;\ s)/2i \sin(\pi s \xi) , \tag{16}$$

which in Dirac delta function notation becomes, by substituting Eq. (14) into Eq. (16),

$$\tilde{W}_s(\xi) = \mathrm{rect}(\Delta x \xi)\left(\left\{X \,\mathrm{sinc}(X\xi) * \sum_{n=-\infty}^{+\infty} \tilde{W}\left(\xi - \frac{n}{\Delta x}\right) 2i \sin\left[\pi s \left(\xi - \frac{n}{\Delta x}\right)\right]\right\} \sum_{m=-\infty}^{+\infty} \delta\left(\xi - \frac{m}{X}\right)\right) \Big/ 2i \sin(\pi s \xi) . \tag{17}$$

Inverse transforming Eq. (17),

$$W_s(x) = \mathfrak{F}_x^{-1}[\tilde{W}_s(\xi)] = \mathfrak{F}_x^{-1}\left[\mathrm{rect}(\Delta x \xi)\left(\left\{X \,\mathrm{sinc}(X\xi) * \sum_{n=-\infty}^{+\infty} \tilde{W}\left(\xi - \frac{n}{\Delta x}\right) 2i \sin\left[\pi s \left(\xi - \frac{n}{\Delta x}\right)\right]\right\} \sum_{m=-\infty}^{+\infty} \delta\left(\xi - \frac{m}{X}\right)\right) \Big/ 2i \sin(\pi s \xi)\right] , \tag{18}$$

and recovery of the wave-front shape can be achieved from an appropriately spaced lattice of the samples values from the wave-front shearing interferogram. The recovery is accomplished by appropriate filtering in the spatial frequency domain and inverse transforming of the filtered array.

HYPOTHETICAL DATA CASE

A hypothetical lateral shearing interferogram was mathematically constructed so that the Fourier data reduction technique could be evaluated. The case considered is applicable to the measurement of an optical wave-front shape after propagation over a long path through a turbulent medium, such as a $\Delta\phi$ record of the type obtained from the experimental technique of Shannon *et al.*[19]

A random aberration function was constructed as the initial step in the generation of the interferogram. The statistical characteristics of the aberration function were appropriately chosen to approximate a possible atmospheric stochastic process. In order to provide a numerical example, an expression for the autocorrelation function of the random process must be assumed. In the case of phase variations, there is no reason to assume that that the function does not fall off monotonically. A Gaussian function could be used, but this function falls off too quickly to be realistic. Therefore, an array of uncorrelated normal deviates, $g(I)$, was convolved with a hyperbolic secant function $\mathrm{sech}(I + n)$ for $n = 1,\ N$, which is as easy to handle, but falls off at a slower rate. The resulting array, $w(n)$, was adjusted for zero mean and a standard deviation of a quarter wavelength. A portion of this aberration function, smoothed between the discrete data points, is shown in Fig. 2 and its autocorrelation function is shown in Fig. 3.

The lateral shearing interferogram was constructed by calculating the inherent phase difference due to the shear s at a distance y from a point source propagating in a homogeneous medium, and adding in the phase difference due to the aberration function in a line x in the record, as shown in Fig. 4.

With the refractive index of the homogeneous medium approximated by one, the pathlength to the point $x_1 = x + s/2$ is by the Pythagorean theorem,

$$R_1 = y[1 + (x + s/2)^2/y^2]^{1/2} . \tag{19}$$

For $(x + s/2)/y \ll 1$, a binomial expansion of Eq. (19) results in

$$R_1 \approx y\left(1 + \frac{(x + s/2)^2}{2y^2}\right) . \tag{20}$$

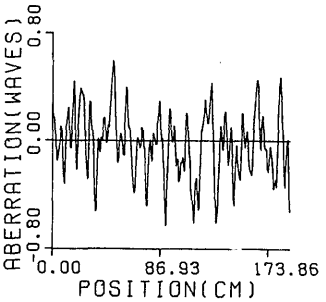

FIG. 2. Input aberration function.

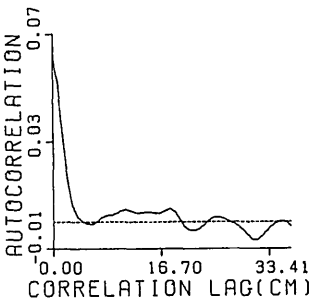

FIG. 3. Input autocorrelation function.

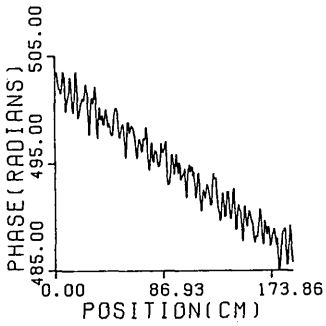

FIG. 5. Lateral shearing interferogram.

Similarly, the pathlength for the point $x_2 = x - s/2$ is

$$R_2 \approx y\left(1 + \frac{(x - s/2)^2}{2y^2}\right) \quad . \tag{21}$$

Therefore the phase difference $\Delta\phi$ due to propagation in the homogeneous medium is

$$\Delta\phi \approx \frac{2\pi(R_2 - R_1)}{\lambda} \approx \frac{-2\pi s x}{\lambda y} = \frac{-2\pi s}{\lambda} \tan\theta \quad . \tag{22}$$

An array of $\Delta\phi(n\Delta x)$ was then combined with the aberration function array, $w(n)$. A quadratic interpolation routine was used to calculate the value of the aberration function at the positions $x + s/2$ and $x - s/2$ for all values, $n = 1, 1024$, of the array. Designating these interpolated values of the aberration function as δ_1/λ and δ_2/λ, the resulting lateral shearing interferogram can be written as,

$$V_s(x, y; s) = W(n\Delta x + s/2, y) - W(n\Delta x - s/2, y)$$

$$= \frac{2\pi}{\lambda}(R_1 - R_2 + \delta_1 - \delta_2) \, , \tag{23}$$

and approximates wave propagation in a turbulent media. A portion of the sheared interferogram with a shear $s = 1$ cm, a sampling interval $\Delta x = 0.75$ cm, a wavelength $\lambda = 5.0 \times 10^{-5}$ cm, at a distance $y = 1.5 \times 10^6$ cm along a line from $x = 6000 - 5808$ cm from the origin is shown in Fig. 5. A computer program was used to generate the interferogram.

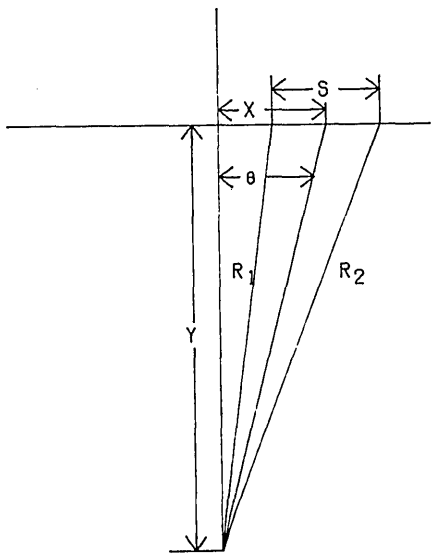

FIG. 4. Interferogram construction.

A second computer program was used to recover the wave-front aberrations from the lateral sheared interferogram. The initial step in this Fourier data reduction program is a straight line least square fit to the lateral shearing interferometric data, $V_s(x, y; s)$, represented by Eq. (23), and a calculation of residuals, $V_{sR}(x, y; s)$, of the fit. This first-order fit of the data is justified by the approximation given in Eq. (22) and removes the phase difference in the interferogram due to propagation in a homogeneous medium.

The residuals are then scaled by Δx to conform to the similarity theorem.[20] The real array $\Delta x V_{sR}(x, y; s)$ is now used to form the complex array $[\Delta x V_{sR}(x, y; s), 0]$ for input into a fast Fourier transform subroutine, and the array is transformed.

Since the original array is real, the resulting transformed complex array $\tilde{V}_{sR}(\xi, y; s)$ is Hermitian,[20] and therefore its real part is even and its imaginary part is odd. Consequently, the nth member of this array, (R, I), with spatial frequency, ξ_n, is related to the $(N + 2 - n)$th member of the array, $(R, -I)$, with spatial frequency, $-\xi_n$, if the complex array has N components. The $(N/2 + 1)$th member of the array has a spatial frequency associated with it of $\xi = \pm 1/2\Delta x$. The modulus of the transformed array is shown in Fig. 6 and demonstrates that Δx has been chosen sufficiently small in order to prevent significant aliasing in the frequency domain.

The transformed complex array $\tilde{V}_{sR}(\xi, y; s)$ is then filtered by multiplication with the complex array $[0, -1/2\sin(\pi s\xi)]$ to obtain the equivalent of Eq. (17). This imaginary filter function is shown in Fig. 7. Since the filter is odd and imaginary, this filter operation results in an anti-Hermetian array, where the real-even and imaginary-odd components of $\tilde{V}_{sR}(\xi, y; s)$ have been

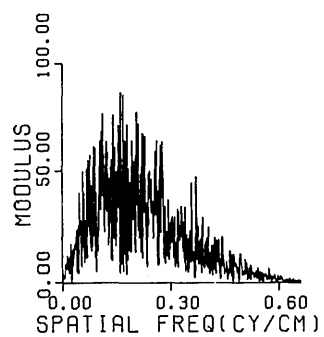

FIG. 6. Modulus of transformed residuals.

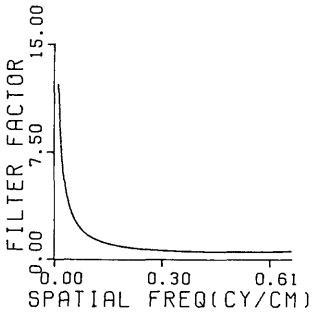

FIG. 7. Imaginary filter function.

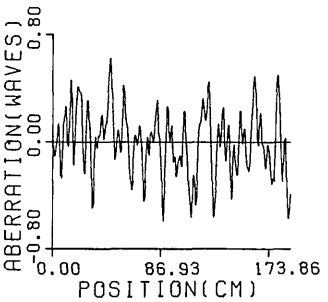

FIG. 9. Recovered aberration function.

interchanged by the filtration. The filter operation at zero frequency is explained in the Appendix. The result of this filtration is the Fourier transform of the wave-front aberrations. In order to obtain the power spectrum of the aberration function, the array is multiplied by its complex conjugate and scaled by the length of the record. The resulting power spectrum is shown in Fig. 8.

The filtered array is Fourier transformed and results in a complex array which has only a real component. However, since the fast Fourier transform subroutine only performs a transform and not an inverse transform, the recovered aberration function is of the form $W_s(-x, y)$, and a proper reordering of the array is required, which results in the recovered wave-front aberration. The portion from $x = 6000$ to 5808 cm, corresponding to the part of the original wave-front aberration function in Fig. 2, is shown in Fig. 9, and shows that the recovery is excellent.

The autocorrelation function is then obtained either by Fourier transformation of the power spectrum or by the equation

$$C(\Delta x) = \frac{1}{X_n - |\Delta x|} \times \int_{-(X_n-|\Delta x|)/2}^{(X_n-|\Delta x|)/2} W\left(x - \frac{\Delta x}{2}, y\right) W\left(x + \frac{\Delta x}{2}, y\right) dx \tag{24}$$

where X_n is the length of the record, and is usually not used for lags, Δx, longer than 5%–10% of the length of the record.[25] These two autocorrelation functions are shown in Fig. 10. The agreement between original and recovered autocorrelations is excellent, and the standard deviations differ by only 0.004 waves for the two wave-front functions.

An estimate of the smoothed (average-over frequency) power spectrum[25] $P_i(\xi)$ of the true power spectrum is shown in Fig. 11. This estimate was obtained by Fourier transforming the apparent autocorrelation function

$$C_i(\Delta x) = D_i(\Delta x)\, C(\Delta x)\,, \tag{25}$$

where $C(\Delta x)$ is the autocorrelation function calculated using Eq. (24) for approximately 5% of the record length, and $D_i(\Delta x)$ is the lag window

$$D_0(\Delta x) = \mathrm{rect}\left(\frac{\Delta x}{2X_n}\right)\,. \tag{26}$$

While the modified apparent autocorrelation functions, which are obtained by multiplying $C(\Delta x)$ by $D_i(\Delta x)$, are far from being respectable estimates of the true autocorrelation function, their transforms are very respectable estimates of smoothed values of the true spectral density.

CONCLUSIONS

The Fourier data reduction technique presented here provides a unique new method for interpretation and analysis of lateral shearing interferograms. The method is especially useful since the requirement of evaluation at only shear distances is not required by the technique.

This additional flexibility in data reduction permits more flexibility in the parameters used during the recording of the interferogram. The shear value can be chosen to give optimum fringe spacing, and recording of the sheared aberration differences can be recorded at any equally spaced intervals in the interferogram. The only requirement on the interval spacing is that appreciable aliasing does not occur for the Fourier transform of the sheared wave front. A complete recovery depends on the concept of a band-limited Fourier transform. However, a more realistic requirement is that the magnitude of the modulus at the

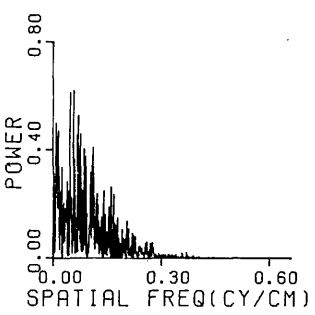

FIG. 8. Power spectrum of wave-front aberrations.

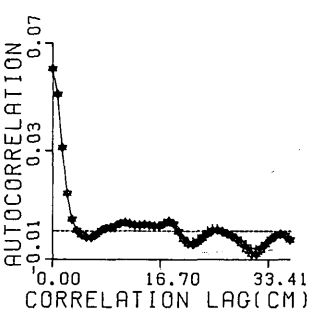

FIG. 10. Output wave-front autocorrelation functions.

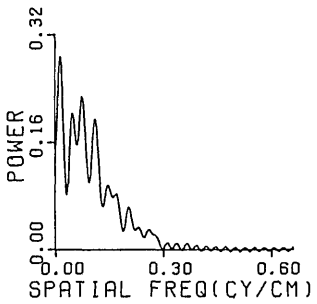

FIG. 11. Smoothed power spectrum.

higher spatial frequencies is negligible compared to its values at the lower spatial frequencies.

This concept can be useful in determining an optimum recording interval for the sheared wave-front interferogram. An interval can be chosen so that appreciable aliasing is just avoided, and this recording interval is then the minimum required for almost complete recovery. This requirement is similar to the concept of efficient recovery in sampling theory.

ACKNOWLEDGMENTS

I am indebted to Roland V. Shack, Optical Sciences Center, University of Arizona, for his encouragement and generous assistance during the course of this study. It was his realization of the representation of a lateral shearing interferogram as a convolution of the wave-front shape with an odd-impulse pair function which inspired the development of this data reduction technique.

APPENDIX

In the derivation of the Fourier data reduction technique, a problem was encountered in dividing Eq. (14) by zero at $\xi = \pm n/s$, $n = 0, 1, 2, \ldots, N$. The solution to this difficulty is now considered.

The laterally sheared interferometric data, $V(x, y; s)$, is a real function. Therefore its Fourier transform can be expressed as

$$\tilde{V}(\xi, y; s) = \int_{-\infty}^{+\infty} V(x, y; s)\cos(2\pi\xi x)\,dx - i \times \int_{-\infty}^{+\infty} V(x, y; s)\sin(2\pi\xi x)\,dx . \tag{A1}$$

Since any function can be split unambiguously into odd and even parts, then

$$V(x, y; s) = O(x, y; s) + E(x, y; s) , \tag{A2}$$

and Eq. (A1) can be written as

$$\tilde{V}(\xi, y; s) = \int_{-\infty}^{+\infty} E(x, y; s)\cos(2\pi\xi x)\,dx - i \times \int_{-\infty}^{+\infty} O(x, y; s)\sin(2\pi\xi x)\,dx , \tag{A3}$$

where the first integral is a real and even and the second integral is an imaginary and odd function of ξ.

Dividing Eq. (A3) by the filter function, $2i\sin(\pi s\xi)$,

$$\tilde{W}(\xi, y) = \frac{-1}{2\sin(\pi s\xi)} \int_{-\infty}^{+\infty} O(x, y; s)\sin(2\pi\xi x)\,dx - \frac{i}{2\sin(\pi s\xi)} \int_{-\infty}^{+\infty} E(x, y; s)\cos(2\pi\xi x)\,dx . \tag{A4}$$

Since the imaginary term of Eq. (A4) is now an odd function of ξ, its value at the origin is zero as far as an inverse transformation is concerned. Therefore taking the limit as $\xi \to 0$ of Eq. (A4),

$$\tilde{W}(\xi, y)_{\xi=0} = -\frac{1}{2}\lim_{\xi\to 0}\left(\frac{1}{\sin(\pi s\xi)} \int_{-\infty}^{+\infty} O(x, y; s)\sin(2\pi\xi x)\,dx\right) \tag{A5}$$

and since the integral is not dependent on ξ, Eq. (A5) can be rearranged to obtain

$$\tilde{W}(\xi, y)_{\xi=0} = -\frac{1}{2} \int_{-\infty}^{+\infty} O(x, y; s)\lim_{\xi\to 0}\left(\frac{\sin(2\pi\xi x)}{\sin(\pi s\xi)}\right) dx . \tag{A6}$$

Invoking L'Hospital's rule, Eq. (A6) becomes

$$\tilde{W}(\xi, y)_{\xi=0} = -\frac{1}{s} \int_{-\infty}^{+\infty} xO(x, y; s)\,dx . \tag{A7}$$

But by the moment theorem,[20] if $f(x)$ has a Fourier transform $\tilde{f}(\xi)$, then the first moment of $f(x)$ is equal to $-(2\pi i)^{-1}$ times the slope of $\tilde{f}(\xi)$ at $\xi = 0$; that is

$$\int_{-\infty}^{+\infty} xf(x)\,dx = [\tilde{f}'(0)/-2\pi i] . \tag{A8}$$

Therefore, using the relationship of Eq. (A8) in Eq. (A7), we obtain

$$\tilde{W}(\xi, y)_{\xi=0} = [\tilde{O}'(0)/2\pi i s] , \tag{A9}$$

where $\tilde{O}'(0)$ is the slope of the Fourier transform of the odd part of the wave-front difference function, $\tilde{O}(\xi)$, at $\xi = 0$. The value of the right hand of Eq. (A9) is real since the transform of a real and odd function is imaginary and odd, and the i in the denominator will cancel. Since the imaginary term of Eq. (A4) was shown to be zero at the origin as far as any inverse transformation is concerned, the evaluation of the indeterminate relationship in Eq. (A5) results in a determinate complex number, $[\tilde{O}'(0)/2\pi i s, 0]$.

Now, $\tilde{O}(\xi)$, at $\xi = 0$, determines the d.c. value of the wave-front aberration function. However, the absolute value of phase is of no consequence in the evaluation of the aberration function. Therefore, when filtration with $2i\sin(\pi s\xi)$ is performed at $\xi = 0$, a proper value for $W_s(0, y)$ in Eq. (18) is the complex number (0, 0).

This approach to the filtering operation at zero spatial frequency was successfully used in the recovery of the wave-front aberration function for the hypothetical data case presented here.

The above argument can not be used for $\xi = \pm n/s$, $n = 1, 2, 3, \ldots, N$. Two alternatives are possible, however. A sampling interval, Δx, can be chosen so that the cutoff of the fast Fourier transform subroutine, $\xi = \pm 1/2\Delta x$, is such that $s/2\Delta x < 1$, and filter values are with the first half cycle of the sine function. This is what was done for the hypothetical data case presented

here. Or, a Δx can be chosen, so that for all members of the array, $\xi \neq \pm n/s$, $n = 1, 2, \ldots, N$. Therefore the indeterminate, 0/0, is not encountered, and all divisions in the array by filtration are possible.

*This research is based on a thesis submitted to the Optical Sciences Center of the University of Arizona in partial fulfillment of the requirements for the M. S. degree.

[1]W. J. Bates, "A Wavefront Shearing Interferometer," Proc. Phys. Soc. 59, 940 (1947).

[2]L. C. Martin, *Technical Optics II* (Sir Isaac Pitman & Son, London, 1961), pp. 330–334.

[3]O. Bryngdahl, in *Progress in Optics IV*, edited by E. Wolf (North Holland, Amsterdam, 1965), pp. 39–47.

[4]J. B. Saunders, "A Wavefront Shearing Interferometer," J. Res. Nat. Bur. Stand., 65, 239 (1961).

[5]J. B. Saunders in *Advanced Optical Techniques*, edited by A. C. S. Van Heel (North Holland, Amsterdam, 1967), pp. 16–20.

[6]J. B. Saunders, "A Simple Interferometer Method for Workshop Testing of Optics," Appl. Opt. 9, 1623 (1970).

[7]R. B. Herrick and J. R. Meyer-Arendt, "Interferometry through the Turbulent Atmosphere at an Optical Path Difference of 354 m," Appl. Opt. 5, 981 (1966).

[8]A. L. Buck, "Effects of the Atmosphere on Laser Beam Propagation," Appl. Opt. 6, 703 (1967).

[9]M. Carnevale, B. Crosignani, and P. Di Porto, "Influence of Laboratory Generated Turbulence on Phase Fluctuations of a Laser Beam," Appl. Opt. 7, 1121 (1968).

[10]M. Bertolotti, M. Carnevale, B. Crosignani, and P. Di Porto, "Influence of Thermal Turbulence in a Convective Ascending Stream on Phase Fluctuations of a Laser Beam," Appl. Opt. 8, 1111 (1969).

[11]M. Bertolotti, L. Muzii, and D. Sette, "Correlation Measurements on Partially Coherent Beams by Means of an Integration Technique," J. Opt. Soc. Am. 60, 1603 (1970).

[12]M. Bertolotti, M. Carnevale, L. Muzii, and D. Sette, "Reversing-Front Interferometer for Phase Correlations Measurements in the Turbulent Atmosphere," Appl. Opt. 9, 510 (1970).

[13]P. Burlamacchi, A. Consortini, and L. Ronchi, "Time-Resolved Measurements of the Phase Fluctuations of a Coherent Beam at the Emergence from a Turbulent Layer," Appl. Opt. 6, 1273 (1967).

[14]R. C. Ward and G. V. Berry, "Differential-Interferometer Seeing Meter," Appl. Opt. 6, 1136 (1967).

[15]K. E. Erickson, "Long Path Interferometry Through an Uncontrolled Atomosphere," J. Opt. Soc. Am. 52, 781 (1962).

[16]M. Bertolotti, M. Carnevale, L. Muzii, and D. Sette, "Interferometric Study of Phase Fluctuations of a Laser Beam Through the Turbulent Atomosphere," Appl. Opt. 7, 2246 (1968).

[17]M. Bertolotti, M. Carnevale, B. Daino, and D. Sette, "Optical Processing in the Phase Correlation Induced by a Turbulent Medium in a Laser Beam," Appl. Opt. 9, 962 (1970).

[18]S. F. Clifford, G. M. B. Bouricius, G. R. Ochs, M. H. Ackley, "Phase Variations in Atmospheric Optical Propagation," J. Opt. Soc. Am. 61, 1279 (1971).

[19]R. R. Shannon and W. S. Smith, "An Experiment for Measuring Effect of Atmospheric Turbulence on a Vertical Optical Path," Proc. SPIE 75, 44 (1976).

[20]R. Bracewell, *The Fourier Transform and its Applications* (McGraw-Hill, New York, 1965).

[21]J. W. Cooley, P. A. W. Lewis, and P. P. Welch, "The Fast Fourier Transform and its Applications," IEEE Trans. Educ. 12, 27 (1969).

[22]E. T. Whittaker, "On the Functions Which are Represented by the Expansions of the Interpolation Theory," Proc. R. Soc. Edinburgh Sect. A, 35, 181 (1915).

[23]C. E. Shannon, "Communication in the Presence of Noise," Proc. IRE 37, 10 (1949).

[24]D. A. Linden, "A Discussion of Sampling Theorems," Proc. IRE 47, 1219 (1959).

[25]R. B. Blackman and J. W. Tukey, The Measurement of Power Spectra (Dover, New York, 1959).